Title

Longitudinal MR spectroscopy to detect progression in patients with lower-grade glioma in the surveillance phase.

Journal

Neuro-oncology advances, 4(1)

ISSN

2632-2498

Authors

Avalos, Lauro N
Luks, Tracy L
Gleason, Tyler
et al.

Publication Date

2022

DOI

10.1093/noajnl/vdac175

Peer reviewed

Neuro-Oncology Advances
4(1), 1–9, 2022 | https://doi.org/10.1093/noajnl/vdac175 | Advance Access date 16 November 2022

Longitudinal MR spectroscopy to detect progression in patients with lower-grade glioma in the surveillance phase

Lauro N. Avalos, Tracy L. Luks, Tyler Gleason, Pablo Damasceno, Yan Li, Janine M. Lupo, Joanna Phillips, Nancy Ann Oberheim Bush, Jennie W. Taylor, Susan M. Chang, and Javier E. Villanueva-Meyer

Department of Radiology and Biomedical Imaging, University of California San Francisco, San Francisco, California 94143, USA (L.N.A., T.L.L., T.G., P.D., Y.L., J.M.L., J.E.V.-M.); Department of Pathology, University of California San Francisco, San Francisco, California 94143, USA (J.P.); Department of Neurological Surgery, University of California San Francisco, San Francisco, California 94143, USA (J.P., N.A.O.B., J.W.T., S.M.C.)

Corresponding Author: Javier Villanueva-Meyer, MD, Department of Radiology and Biomedical Imaging, Box 0628, Floor P1, Room C-09H, San Francisco, CA 94143-0628, USA (Javier.Villanueva-Meyer@UCSF.edu).

Abstract

Background. Monitoring lower-grade gliomas (LrGGs) for disease progression is made difficult by the limits of anatomical MRI to distinguish treatment related tissue changes from tumor progression. MR spectroscopic imaging (MRSI) offers additional metabolic information that can help address these challenges. The goal of this study was to compare longitudinal changes in multiparametric MRI, including diffusion weighted imaging, perfusion imaging, and 3D MRSI, for LrGG patients who progressed at the final time-point and those who remained clinically stable.

Methods. Forty-one patients with LrGG who were clinically stable were longitudinally assessed for progression. Changes in anatomical, diffusion, perfusion and MRSI data were acquired and compared between patients who remained clinically stable and those who progressed.

Results. Thirty-one patients remained stable, and 10 patients progressed. Over the study period, progressed patients had a significantly greater increase in normalized choline, choline-to-*N*-acetylaspartic acid index (CNI), normalized creatine, and creatine-to-*N*-acetylaspartic acid index (CRNI), than stable patients. CRNI was significantly associated with progression status and WHO type. Progressed astrocytoma patients had greater increases in CRNI than stable astrocytoma patients.

Conclusions. LrGG patients in surveillance with tumors that progressed had significantly increasing choline and creatine metabolite signals on MRSI, with a trend of increasing T2 FLAIR volumes, compared to LrGG patients who remained stable. These data show that MRSI can be used in conjunction with anatomical imaging studies to gain a clearer picture of LrGG progression, especially in the setting of clinical ambiguity.

Key Points

- Progressed LrGG patients had greater increases in multiple metabolic markers than stable patients.
- MRSI can be used in conjunction with anatomical imaging studies to gain a clearer picture of LrGG progression, especially in the setting of clinical ambiguity.

Lower-grade gliomas (LrGGs) are either WHO grade 2 and 3 astrocytomas (isocitrate dehydrogenase (IDH)-mutant) or WHO grade 2 oligodendrogliomas (IDH-mutant with chromosome 1p/19q co-deletion), that can be differentiated from higher-grade gliomas (WHO grade 4, astrocytoma, IDH-mutant and the more common glioblastoma; WHO grade 3 oligodendrogliomas) by their unique histological features.[1] Advances in molecular characterization of these tumors have

Importance of the Study

The goal of this study was to compare longitudinal changes in multiparametric MRI, including diffusion weighted imaging, perfusion imaging, and 3D MRSI, for LrGG patients in surveillance with tumors that progressed and those who remained clinically stable. LrGG patients that progressed had significantly increasing choline and creatine metabolite signals on MRSI, with a trend of increasing T2 FLAIR volumes, compared to LrGG patients who remained stable. Together, these data show that MRSI can be used in conjunction with anatomical imaging to gain a clearer picture of lower-grade glioma progression, especially in the setting of clinical ambiguity.

clarified classification opening up new avenues for potential targeted treatments that could lead to improvements in treatment paradigms, increased survival, and reduced morbidity for long term survivors.[2,3] While the ability to delay radiation and chemotherapy is important for reducing side effects and optimizing quality of life, the relatively slow rate of change in lesion volume and lack of specificity from standard imaging methods, such as the Brain Tumor Imaging Protocol, hinders the identification of an optimal time point for initiating a new treatment.[4] Further, standard imaging methods are not able to predict which patients will experience stable disease, progression, or a favorable response to therapy.[5,6]

Determination of tumor growth in LrGG is highly dependent on imaging technique, which is likely to vary given the long-time course over which LrGG patients are followed and the heterogeneity of treatment. LrGGs are also often irregular in shape due to their infiltrative growth pattern and can be further distorted by treatment effects (eg, post-surgical gliosis, radiotherapy related changes, edema), which can impair accurate measurements of tumor size from linear 2D measurements with T2 FLAIR being the standard surveillance modality for LrGG typically showing non-enhancing tumor growth. Further, 2D measurements of tumor size over serial MR exams for slow growing tumors can be affected by technical factors such as variations in slice orientation, acquisition parameters, or scanner type. These characteristics of LrGGs and their imaging can lead to significant inter-observer and intra-observer variability in tumor measures when using a 2D product method to estimate tumor size.[7,8] Thus, there is a need for more sensitive imaging predictors of tumor growth and alternative measures of treatment response.

Multiparametric MR examinations that integrate conventional anatomic imaging with more advanced imaging techniques such as diffusion weighted imaging (DWI), perfusion imaging, and magnetic resonance spectroscopic imaging (MRSI) have been developed to provide a more comprehensive evaluation of the structural, physiologic, and metabolic properties of LrGGs. To date, these advanced imaging techniques have been primarily studied in the evaluation of suspected newly diagnosed LrGG to assist with targeting for tissue sampling and in non-invasive diagnosis.[9] The discovery of IDH mutation status as an important differentiator of glioma classification has afforded detection of its metabolite 2-hydroxyglutarate (2HG) using MRSI.[10] While recent studies have supported its use as a biomarker for metabolic activity in lower-grade glioma,[11] the technical and tumor volume requirements for 2HG measurement limit its current clinical utility, and emphasize the continued need for multiparametric MRI biomarkers of progression in LrGG.

The goal of this study was to compare longitudinal changes in multiparametric MRI, including DWI, perfusion imaging, and 3D MRSI, for LrGG patients who progressed at the final timepoint and those who remained both clinically and radiographically stable. We hypothesized that these techniques would be valuable in the serial evaluation of LrGGs undergoing surveillance and would offer additional information beyond conventional anatomic imaging in identifying tumor progression.

Methods

Patients

This study included histologically confirmed LrGG patients who were clinically stable and off treatment (ie, surgery, radiation, chemotherapy). There was no upper limit on the time between completed treatment and enrollment, or the number and types of previous treatments. Clinical stability was determined by the referring neuro-oncologist which included patients that recently received surgery and no further therapies. Eligible patients needed to be over 18 years old, have a Karnofsky performance status (KPS) ≥ 70, and be fluent in English. All participants gave written informed consent, and ethical approval was granted by the UCSF Institutional Review Board, in compliance with the Helsinki Declaration.

Clinical and Demographic Variables

Clinical and demographic data were collected by review of patients' electronic medical records. This included age, education, time since diagnosis/surgery, previous treatment, tumor grade, extent of resection (biopsy, subtotal, gross total), KPS and use of anti-epileptic drugs (AEDs). Patients were classified according to the 2021 WHO central nervous system classification integrated diagnoses: astrocytoma, IDH-mutant; oligodendroglioma, IDH-mutant and 1p19q co-deleted; and NOS (not otherwise specified: molecular status unknown). IDH mutation status and co-deletion of

1p19q were determined by immunohistochemistry and FISH, respectively. MRI was performed at intervals according to the treating neuro-oncologist recommendations ranging from every 3–6 months depending on point in disease course.[1,7] Serial MRIs were performed for each patient until the time of progression or until the time the dataset was locked for analysis.

Clinical Definition of Progression

Progression was determined by the treating neuro-oncologist with or without consensus of multidisciplinary tumor board, based on change in the T2 FLAIR or T1 contrast-enhancing lesions, or new or worsening neurological symptoms, with a recommendation for a change in treatment.

MRI Acquisition

All scans were performed on a GE Discovery 750 3T canner (GE Healthcare, Waukesha, WI) with a 32-channel head coil (Nova Medical, Wilmington, MA). Standard anatomical imaging included 3D T2-weighted Fluid Attenuated Inversion Recovery (FLAIR), 2D T2-weighted fast spin echo, and 3D T1-weighted pre- and post-gadolinium sequences. DWI was obtained in the axial plane with 24 gradient directions [repetition time (TR)/echo time (TE) = 1000/108 ms, voxel size = 1.7 × 1.7 × 3 mm, b = 1000 s/mm]. Dynamic susceptibility contrast-enhanced (DSC) perfusion images were acquired before, during, and following a 5 ml/s bolus injection of 0.1 mmol/kg body weight gadolinium diethyltriamine pentaacetic acid (Gd-DTPA) using a series of T2*-weighted echo-planar images [TR/TE/Flip-angle = 1500/35 ms/30–35°, 128 × 128 matrix, slice thickness = 3–4 mm, 20–25 slices with 80 time points].

MRSI Acquisition Using Atlas-Based Prescription

Our MRSI method predefines the prescription on a standard image atlas and transforms both the selected volume and outer volume suppression bands to individual subject space during each scan session.[12]This allows a fully automated prescription that covers the desired anatomy consistently for different time points in a single subject.[13] In each scan session, the atlas T1-weighted image was aligned to the 3D T1 image volume of the subject, and the predefined MRSI volume and outer volume suppression bands were transformed by applying the transformation matrix resulting from the alignment. Higher order shimming was performed to reduce the degree of magnetic field in homogeneity. Immediately after the field shimming, the 3D multi-voxel H-1 MRSI was acquired with point resolved spectroscopy (PRESS) volume selection, chemical shift selective (CHESS) water suppression, phase encoding in two dimensions and flyback encoding in the superior–inferior direction.[12] The sequence parameters were as follows: TE/TR 144/1250 ms, phase encoding grid 18 × 18 × 16, nominal resolution 1cm,[3] total acquisition time 11 min. An over excitation factor of PRESS volume 1.2 was used to reduce chemical shift misregistration.[14]

MR Data Processing

The anatomic, diffusion, perfusion and spectroscopic images were aligned to the T1 post-contrast image using FMRIB's Linear Image Registration Tool.[15,16] Each region of interest (ROI) was defined by a single investigator with the guidance of UCSF neuroradiologists. The T2 lesion ROI was defined using semi-automated software (3DSlicer) to include all T2 FLAIR hyperintensity relative to the surrounding normal tissue. These T2 lesion ROIs are 3D volumetric ROIs that include all T2 FLAIR hyperintensity on all slices. A contrast-enhancing lesion ROI was defined when contrast-enhancement was present.

A previously published algorithm was applied to estimate relevant DWI parameters and normalize between field strengths using estimates from normal appearing brain tissue.[17] To provide metrics that described regions with abnormal intensities, the voxel values for ADC and FA maps were first normalized to the mode of intensities in normal appearing brain tissue (calculated across the entire cerebrum, excluding the T2 lesion ROI). Percentiles (10th, 50th, 90th) were then calculated from histograms of normalized intensities within T2 lesion ROIs.

Perfusion imaging data, including cerebral blood volume (CBV) and peak height (PH), were calculated for each voxel using software developed in our research group.[18–20] The T2* signal-intensity time curves acquired during the first-pass of the gadolinium bolus were converted to change in the relaxation rate (DR2*). PH was defined as the maximum DR2* value of the first-pass curve. CBV maps were calculated on a voxel-by-voxel basis utilizing a modified gamma-variate function that considers leakage of the contrast agent.[19] The CBV and PH values from the T2 FLAIR lesions were normalized by the median value of the histogram derived from normal brain tissue.[21,22]

MRSI data acquisition was conducted using fully automated reconstruction and post-processing described in previous publications.[13,14,23] In brief, the start point was the raw data file obtained from the lactate-edited MRSI sequence. This comprised interleaved acquisitions (or cycles) obtained with radiofrequency pulses that modulated the phase of the lactate peak, with each cycle having 8-channels of data corresponding to the multiple receiver coils. The k-space time domain data for each cycle and channel were first filtered with a 4-Hz exponential function in the time domain, zero filled to 1024 points, and Fourier transformed to produce a k-space array of spectra. The next step was to apply the k-space Fourier transforms to produce 3D spatial arrays of spectral data, followed by combination using in-house developed software that weights the data by coil sensitivities estimated from low resolution proton density weighted images.[13] Additional phase corrections were applied in the SI dimension to account for the flyback echo-planar readout gradient.[24]The cycles were summed to produce an array of spectra containing choline (Cho), creatine (Cr), NAA (N-Acetylaspartic acid), and lipid and subtracted to produce an array of spectra containing lactate. Spectra were baseline subtracted and phase and frequency corrected using parameters estimated from the summed array.

Peak heights and areas were determined from baseline subtracted, frequency and phase corrected spectra on a

voxel-by-voxel basis.[25] Metabolite PHs were normalized by median PHs in normal brain for choline and creatine (nCho and nCr), and normalized lactate and lipid (nLac, nLip) were estimated by metabolite PHs divided by the median peak NAA intensity in normal brain. The choline-to-NAA index (CNI), a *z*-score that reflects changes in the relative levels of these two metabolites compared to normal brain voxels, and the creatine-to-NAA (CRNI) index and choline-to-creatine (CCRI) index, defined in a similar manner, were computed automatically for each voxel using in-house software.[26]

Statistical Analysis

The relationships among the within-subjects effect of time (days to progression/latest scan), the between-subjects effect of WHO type (histological and molecular integrated diagnosis), and MRI parameters were assessed with repeated-measures analyses of variance (using JMP Pro 13.0, SAS Institute Inc). The cut-off for defining a significant result was a *P* value of .05, with a Benjamini-Hochberg False Discovery Rate correction for multiple comparisons.[27] Significant main effects for three-way interactions were followed up with pairwise Tukey-Kramer tests.

Results

Patient Characteristics

Our study cohort included 41 total patients with LrGG, 31 who remained stable throughout the study and 10 who had disease progression. The median age of the population was 45 (range 24–66 years) and 17 (41%) were female. There were 26 patients with astrocytoma, IDH-mutant, 12 patients with oligodendroglioma, IDH-mutant, and

Table 1. Patient demographics

	Progressed	Stable	Progressed vs stable
Age			
Median years	45	44	$F = .86$, $P = .36$
Grade			
2	7	19	Chisq = 25, $P = .62$
3	3	12	
WHO type			
Astrocytoma IDH-mutant	6	20	Chisq = 3.55, $P = .06$
Oligodendroglioma	4	8	
NOS	0	3	
Upgraded at progression			
Yes	2		
No	5		
No surgery	3		
Prior chemotherapy			
No	7	9	Chisq = 5.28, $P = .022$
Yes	3	22	
Prior radiation therapy			
No	8	14	Chisq = 3.93, $P = .048$
Yes	2	17	
Number of prior surgeries			
Median	1	1	$F = .27$, $P = .61$
Mean	1.5	1.4	
Time from diagnosis			
Median days	1184	1856	$F = .5$, $P = .48$
Mean days	1978	2483	
Number of MRI scans			
Median	6	4	$F = 3.75$, $P = .06$
Mean	5.4	4.3	
Presence of T1 contrast-enhancement			
Baseline scan	1	2	ns
Progression/final scan	2	2	

1p/19q-co-deleted, and 3 NOS patients for whom the molecular status was unknown (Table 1). Additional clinical data can be found in Supplementary Table 1.

Volumetrics

The trend towards increasing T2 FLAIR volume over time in progressed patients compared to stable patients did not reach significance (F = 3.64 P = .065) (Table 2, Figure 1). Progressed patients had a greater increase in contrast-enhancing volume over time than stable patients (F = 4.55, P = .039), although only two stable patients and two progressed patients had any contrast-enhancement. Regarding the two patients with contrast-enhancement, in one patient the enhancement was attributed to post-radiation change and was stable over the course of the study and the other patient the enhancement was attributed to post-surgical change and resolved over the course of the study. The remaining 37 patients had no contrast-enhancement at any time-point.

Table 2. MRSI metabolite values for progressed and stable LrGG patients[a]

	Progressed	Stable	F	P
T2 FLAIR Slope (cm^3 per month)				
Mean	0.1678	0.1074	3.64	.065
CNI slope				
Mean	0.0102	−0.0343	5.13	.030
CRNI slope				
Mean	0.0182	−0.0259	5.8	.023
nCHO slope				
Mean	−0.0031	−0.0114	4.12	.050
nCRE				
Mean	0.0052	−0.0121	5.57	.035
nADC				
Mean	0.0092	−0.0052	.05	.827
nCBV				
Mean	0.0044	−0.0250	1.76	.193

[a]In Table, we present the mean slopes, but the statistical analysis is a repeated-measures analysis of variance looking at the effect of time across each imaging time-points within each patient, and the F and P values correspond to that analysis. The mean slope is a summary statistic included to capture the patterns of group change over time.

Diffusion Weighted and Perfusion Imaging

There were no significant differences between progressed and stable patients in change over time for any diffusion or perfusion measures. Across all patients, normalized CBV (nCBV) decreased over time (F = 5.19, P = .028). There was also a significant interaction between progression status and WHO diagnosis on nCBV that did not vary over time (F = 5.5, P = .025) Although post-hoc assessments in oligodendroglioma patients did not reach significance, those who progressed had higher nCBV than stable patients (F = 3.86, P = .076), whereas astrocytoma progressed patients had no difference in nCBV from stable astrocytoma patients (F = 1.6, P = .22).

MRSI

Progressed patients had a greater increase in CNI, nCho, CRNI, and nCre over time than stable patients (F = 5.13, P = .03; F = 4.12, P = .05; F = 5.8, P = .023; and F = 5.57, P = .025, respectively) (Figure 1). There was also a significant three-way interaction between change in CRNI over time, progression status and WHO type (astrocytomas vs oligodendrogliomas, NOS patients excluded) (F = 9.72, P = .005). In astrocytomas, progressed patients had a greater increase in CRNI over time than stable patients (F = 14.2, P = .0012), while in oligodendrogliomas, the

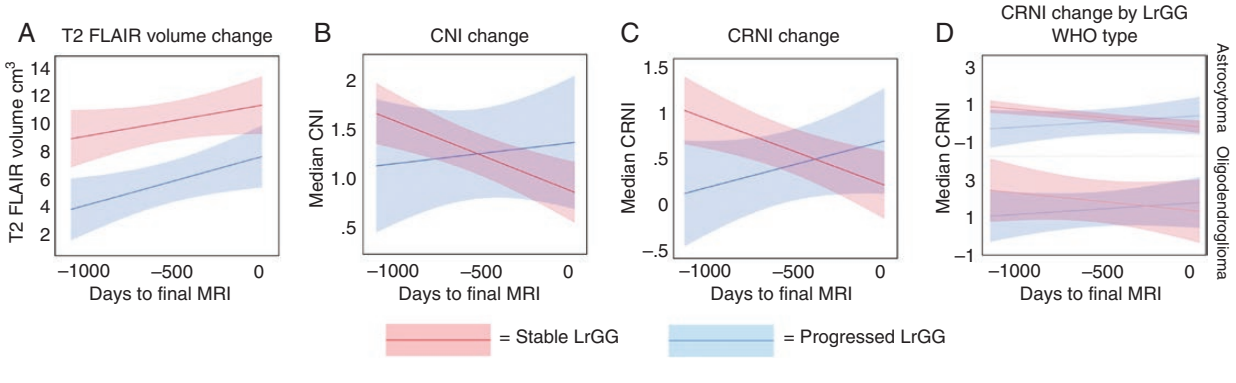

Figure 1. Mean slope of change over time in progressed and stable LrGG patients for (a) T2 FLAIR lesion volume, (b) the choline-to-NAA index (CNI) within the T2 FLAIR lesion, (c) the creatine-to-NAA (CRNI) index within the T2 FLAIR lesion, and (d) the CRNI by WHO type [3 Not Otherwise Specified tumors (NOS) were excluded]. Over time, LrGG patients who progressed at the final timepoint had significantly increasing CNI and CRNI, compared to patients who remained stable. Progression was defined as significant growth in the T2 FLAIR or T1 contrast-enhancing lesions since prior treatment, or new or worsening neurological symptoms, with a recommendation for a change in treatment.

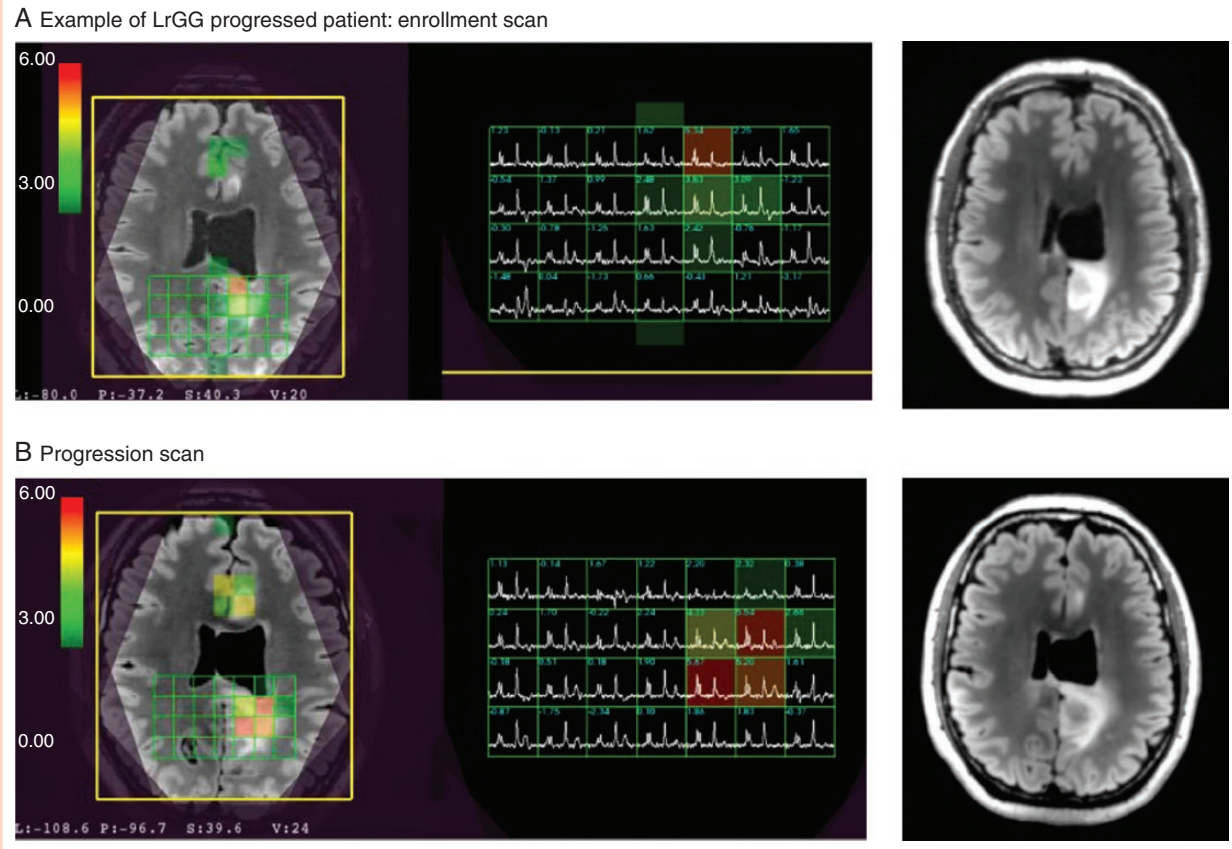

Figure 2. Example of 3D Lactate-edited 1H MRSI for a Progressed patient with LrGG at the time of (a) study enrollment and (b) progression. The Cho-to-NAA index (CNI) overlaid on T2 FLAIR weighted images shows that the extent of abnormal metabolic lesion has increased at the time of progression. The patient was a 48-year-old male with a grade 2 Astrocytoma, IDH-mutant.

difference between progressed and stable patients was not significant (F = .45, P = .51). Although nLip and nLac decreased over time across all patients (F = 5.6. P = .023; F = 14.73 P = .0005), progressed patients had significantly higher levels of nLip (F = 9.87, P = .004) and nLac (F = 5.18, P = .03) compared to stable patients, regardless of time-point. Figures 2 and 3 show example metabolite spectra for a patient that progressed and a patient that remained stable, respectively.

Discussion

In this study, we found 3D MRSI characteristics of post-treatment LrGG in surveillance that significantly increased over time in patients who progressed, compared to patients who remained stable. Overall, our findings build upon a growing body of evidence that routine MRSI in LrGG provides prognostic value through its unique capability to measure local metabolic activity, indicating tumor changes that can guide management. T2 FLAIR volume increase, the primary indicator of clinical progression in LrGG,[4] can be subtle and non-specific in LrGG patients undergoing post-treatment surveillance. In this study, both progressed and stable LrGGs showed T2 FLAIR volumes increasing over time, and the difference between the groups did not reach significance. Given this ambiguity, MRSI provides unique and complementary information to understand tissue metabolism and characterize subtle morphologic changes. This is particularly relevant in light of recent evidence that highlights the importance of delaying chemotherapy or radiation in LrGG to reduce the risk of malignant transformation through induced hypermutation as well as a preventative measure against lasting effects of chemotherapy and radiation related neurocognitive changes.[28]

Our findings demonstrate the utility of multiple metabolic indicators that showed significant changes leading up to progression. Significantly larger increases in the levels of nCho, choline-to-NAA index, nCre, and creatine-to-NAA index were observed in patients who progressed, compared to those who remained stable. Choline is associated with cell proliferation and altered membrane phospholipid metabolism.The MRSI creatine peak includes both creatine and phosphocreatine, and is a marker of cellular metabolism, while NAA is a marker of normal brain tissue and actively functioning neurons helpful in most brain tumors classes.

Despite the small number of patients studied, CRNI showed a significant increase over time in progressed

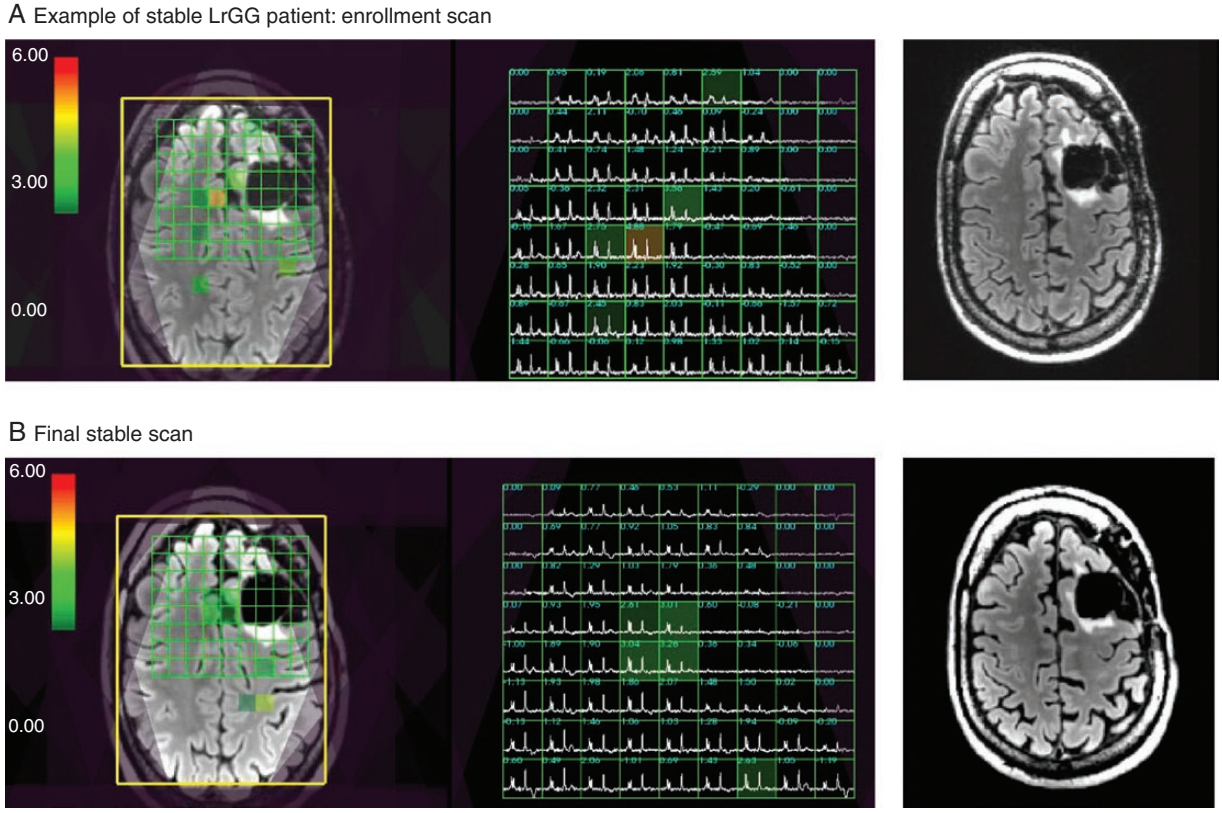

Figure 3. Example of 3D Lactate-edited 1H MRSI for a Stable patient with LrGG at the time of (a) study enrollment and (b) final scan. The Cho-to-NAA index (CNI) overlaid on T2 FLAIR weighted images shows that the extent of abnormal metabolic lesion has not increased over the study period. The patient was a 57-year-old male with a grade 2 Oligodendroglioma, IDH-mutant, 1p19q co-deleted.

astrocytoma compared to stable astrocytoma, an effect that was not significant in oligodendroglioma, suggesting that changes in creatine levels may offer information specific to WHO glioma types. Howe et al. showed that glioblastomas had lower levels of creatine than grade 2 and 3 astrocytomas.[29] Lupo et al[30] found that within abnormal perfusion PH areas of grade 4 gliomas (indicative of leaky blood vessels), reductions in creatine and increases in lactate were observed. Lower creatine within areas of abnormal PH was also observed in grade 3 LrGGs, while areas of elevated CBV had higher creatine, potentially signifying that more energy is needed in the initial recruitment and formation of new vessels. Ozturk-Isik et al[31] reported creatine was reduced in grade 3 LrGG lesions compared to normal appearing white matter, but in areas of high metabolic activity (CNI > 4) within the lesion, creatine was higher. Increased creatine may be an early biomarker of reduced energy reserves from anaerobic respiration before lactate accumulation. We hypothesize that once transformation to a more malignant phenotype occurs, the creatine declines and lactate levels begin to rise, especially in regions with leaky vessels.

Previous cross-sectional studies have shown metabolic differences between oligodendroglioma and astrocytoma using MRSI. Stadlbauer et al[32] found that grade 3 oligodendrogliomas had a significantly lower maximum creatine concentration than grade 3 astrocytomas. Vuori et al[33] reported that grade 2 astrocytomas had lower normalized creatine, and grade 2 oligodendrogliomas had higher normalized creatine, compared with matched controls subjects. Our longitudinal results may offer further insight into creatine's role in glioma metabolism.

The utility of MRSI is exemplified in its ability to depict areas of active tumor metabolism even in the setting of non-specific or inconclusive structural MRI findings. MRSI may direct clinicians to follow suspicious areas of interest or label MRI changes as clinically silent with greater confidence. Caveats of MRSI include the required additional acquisition time per scan, the necessity for an experienced technologist in protocols beyond the typical MRI scan procedures, and the added complexity of post-acquisition processing. To combat this, we have organized a streamlined acquisition process, including atlas-based automatic prescription and fast MRSI acquisitions using flyback echo-planar trajectory in addition to previously published institutional processes.[12,34]

Higher-grade gliomas show DWI alterations, indicating increased cellularity, and increased perfusion, indicating neoangiogenesis and hypervascularity, while LrGGs often do not demonstrate these imaging changes.[17,35–37] We did not find any significant differences in diffusion or perfusion changes over time between the progressed and stable

LrGGs. Across all patients, diffusion metrics remained consistent over time, and nCBV decreased over time. These results suggest that longitudinal monitoring of diffusion and perfusion are not likely to aid in identifying LrGG progression in the setting of inconclusive structural MRI findings.

The limitations of this study include the relatively low numbers of patients with progression, as well as our patients being recruited from a single center. Including more patients will improve our ability to look at the role of MRSI and other advanced imaging parameters to determine progression in particular clinical subgroups of LrGG (eg, astrocytomas with previous radiotherapy and/or chemotherapy vs. those treated solely with surgery). Nonetheless, as treating physicians and clinical scientists, our impact is often measured in incremental improvements and while our data show small, though significant, differences the results provide support for the use of MRSI as an adjunct to often indeterminant imaging and clinical findings surrounding glioma progression.

Research connecting metabolic findings to the cellular and molecular underpinnings of higher-grade glioma biology has previously been done with glioblastoma cells lines, which showed high variability in metabolites as measured by MRSI and cell culture metabolites.[38] A similar study has not been done for LrGGs. Several studies have shown considerable upregulation of genomic and transcriptomic components of gliomas pertaining to metabolic pathway enzymes such as lactate dehydrogenase and creatine kinase with levels increasing with glioma grade.[39,40] Similarly, our results support these data from a metabolic imaging perspective with increased metabolic indexes of creatine and choline. Though we did not conduct a comprehensive enough study to validate these findings, future studies could combine pathology, transcriptomic, and MRSI data to create robust metabolic phenotyping of LrGGs.

Conclusion

This study supports the use of MRSI as an imaging complement to the clinical evaluation of lower-grade glioma progression. LrGG patients in surveillance with tumors that progressed had significantly increasing choline and creatine metabolite signals on MRSI, with a trend of increasing T2 FLAIR volumes, compared to LrGG patients who remained stable. Together, these data show that MRSI can be used in conjunction with anatomical imaging to gain a clearer picture of lower-grade glioma progression, especially in the setting of clinical ambiguity.

Supplementary material

Supplementary material is available online at *Neuro-Oncology Advances* online.

Keywords

lower-grade glioma | magnetic resonance spectroscopic imaging | progression.

Funding

Funding was provided by the LoGlio Collective.

Conflict of Interest: None.

Authorship

Experimental design (TG, LNA, TLL, PD, JEVM)
Experimental implementation (TG, LNA, TLL, JEVM)
Analysis of data (LNA, JEVM, PD, JP)
Interpretation of the data (LNA, TLL, JEVM, PD, NAOB, JWT, SMC, JP)

References

1. Louis DN, Perry A, Wesseling P, et al. The 2021 WHO classification of tumors of the central nervous system: a summary. *Neuro Oncol.* 2021;23(8):1231–1251.
2. Konteatis Z, Artin E, Nicolay B, et al. Vorasidenib (AG-881): a first-in-class, brain-Penetrant dual inhibitor of mutant IDH1 and 2 for treatment of Glioma. *ACS Med Chem Lett.* 2020;11(2):101–107.
3. Chuntova P, Yamamichi A, Chen T, et al. Inhibition of D-2HG leads to upregulation of a proinflammatory gene signature in a novel HLA-A2/HLA-DR1 transgenic mouse model of IDH1R132H-expressing glioma. *J ImmunoTher Cancer.* 2022;10(5):e004644.
4. Ellingson BM, Bendszus M, Boxerman J, et al; Jumpstarting Brain Tumor Drug Development Coalition Imaging Standardization Steering Committee. Consensus recommendations for a standardized Brain Tumor Imaging Protocol in clinical trials. *Neuro Oncol.* 2015;17(9):1188–1198.
5. Upadhyay N, Waldman AD. Conventional MRI evaluation of gliomas. *BJR.* 2011;84(special_issue_2):S107–S111.
6. Villanueva-Meyer JE, Mabray MC, Cha S. Current clinical brain tumor imaging. *Neurosurgery.* 2017;81(3):397–415.
7. Provenzale JM, Ison C, DeLong D. Bidimensional measurements in brain tumors: assessment of interobserver variability. *Am J Roentgenol.* 2009;193(6):W515–W522.
8. Provenzale JM, Mancini MC. Assessment of intra-observer variability in measurement of high-grade brain tumors. *J Neurooncol.* 2012;108(3):477–483.
9. Luks TL, McKnight TR, Jalbert LE, et al. Relationship of in vivo MR parameters to histopathological and molecular characteristics of newly diagnosed, nonenhancing lower-grade gliomas. *Transl Oncol.* 2018;11(4):941–949.
10. Choi C, Raisanen JM, Ganji SK, et al. Prospective longitudinal analysis of 2-hydroxyglutarate magnetic resonance spectroscopy identifies broad clinical utility for the management of patients with IDH-mutant glioma. *J Clin Oncol.* 2016;34(33):4030–4039.
11. Autry AW, Lafontaine M, Jalbert L, et al. Spectroscopic imaging of D-2-hydroxyglutarate and other metabolites in pre-surgical patients with IDH-mutant lower-grade gliomas. *J Neurooncol.* 2022;159(1):43–52.
12. Bian W, Li Y, Crane JC, Nelson SJ. Fully automated atlas-based method for prescribing 3D PRESS MR spectroscopic imaging: toward robust and

reproducible metabolite measurements in human brain. *Magn Reson Med.* 2018;79(2):636–642.

13. Crane JC, Olson MP, Nelson SJ. SIVIC: Open-source, standards-based software for DICOM MR spectroscopy workflows. *Int J Biomed Imag.* 2013;2013:169526.
14. Li Y, Osorio JA, Ozturk-Isik E, et al. Considerations in applying 3D PRESS H-1 brain MRSI with an eight-channel phased-array coil at 3 T. *Magn Reson Imag.* 2006;24(10):1295–1302.
15. Jenkinson M, Bannister P, Brady M, Smith S. Improved optimization for the robust and accurate linear registration and motion correction of brain images. *Neuroimage.* 2002;17(2):825–841.
16. Duarte-Carvajalino JM, Sapiro G, Harel N, Lenglet C. A framework for linear and non-linear registration of diffusion-weighted MRIs using angular interpolation. *Front Neurosci.* 2013;7:41.
17. Wen Q, Jalilian L, Lupo JM, et al. Comparison of ADC metrics and their association with outcome for patients with newly diagnosed glioblastoma being treated with radiation therapy, temozolomide, erlotinib and bevacizumab. *J Neurooncol.* 2015;121(2):331–339.
18. Lee MC, Cha S, Chang SM, Nelson SJ. Dynamic susceptibility contrast perfusion imaging of radiation effects in normal-appearing brain tissue: changes in the first-pass and recirculation phases. *J Magn Reson Imag.* 2005;21(6):683–693.
19. Li Y, Lupo JM, Polley MY, et al. Serial analysis of imaging parameters in patients with newly diagnosed glioblastoma multiforme. *Neuro Oncol.* 2011;13(5):546–557.
20. Lupo JM, Cha S, Chang SM, Nelson SJ. Dynamic susceptibility-weighted perfusion imaging of high-grade gliomas: characterization of spatial heterogeneity. *Am J Neuroradiol.* 2005;26(6):1446–1454.
21. Essock-Burns E, Lupo JM, Cha S, et al. Assessment of perfusion MRI-derived parameters in evaluating and predicting response to antiangiogenic therapy in patients with newly diagnosed glioblastoma. *Neuro Oncol.* 2011;13(1):119–131.
22. Barajas RF, Phillips JJ, Parvataneni R, et al. Regional variation in histopathologic features of tumor specimens from treatment-naive glioblastoma correlates with anatomic and physiologic MR Imaging. *Neuro Oncol.* 2012;14(7):942–954.
23. Nelson SJ, Kadambi AK, Park I, et al. Association of early changes in 1H MRSI parameters with survival for patients with newly diagnosed glioblastoma receiving a multimodality treatment regimen. *Neuro Oncol.* 2017;19(3):430–439.
24. Cunningham CH, Vigneron DB, Chen AP, et al. Design of flyback echo-planar readout gradients for magnetic resonance spectroscopic imaging. *Magn Reson Med.* 2005;54(5):1286–1289.
25. Li Y, Lupo JM, Parvataneni R, et al. Survival analysis in patients with newly diagnosed glioblastoma using pre- and postradiotherapy MR spectroscopic imaging. *Neuro Oncol.* 2013;15(5):607–617.
26. McKnight TR, Noworolski SM, Vigneron DB, Nelson SJ. An automated technique for the quantitative assessment of 3D-MRSI data from patients with glioma. *J Magn Reson Imag.* 2001;13(2):167–177.
27. Benjamini Y, Hochberg Y. Controlling the false discovery rate: a practical and powerful approach to multiple testing. *J R Stat Soc Ser B (Methodological).* 1995;57(1):289–300.
28. Choi S, Yu Y, Grimmer MR, et al. Temozolomide-associated hypermutation in gliomas. *Neuro-Oncology.* 2018;20(10):1300–1309.
29. Howe FA, Barton SJ, Cudlip SA, et al. Metabolic profiles of human brain tumors using quantitative in vivo1H magnetic resonance spectroscopy. *Magn Reson Med.* 2003;49(2):223–232.
30. Lupo JM, Cha S, Chang SM, Nelson SJ. Analysis of metabolic indices in regions of abnormal perfusion in patients with high-grade glioma. *Am J Neuroradiol.* 2007;28(8):1455–1461.
31. Ozturk-Isik E, Pirzkall A, Lamborn KR, et al. Spatial characteristics of newly diagnosed Grade 3 glioma assessed by magnetic resonance metabolic and diffusion tensor imaging. *Transl Oncol.* 2012;5(1):10–18.
32. Stadlbauer A, Gruber S, Nimsky C, et al. Preoperative grading of gliomas by using metabolite quantification with high-spatial-resolution proton MR spectroscopic imaging. *Radiology.* 2006;238(3):958–969.
33. Vuori K, Kankaanranta L, Häkkinen AM, et al. Low-grade gliomas and focal cortical developmental malformations: differentiation with proton MR spectroscopy. *Radiology.* 2004;230(3):703–708.
34. Crane JC, Li Y, Olson MP, et al. Automated prescription and reconstruction of brain MR spectroscopy data for rapid integration into the clinical workflow. *Neurol Disord Epilepsy J.* 2017;1(1):111.
35. Hilario A, Sepulveda JM, Perez-Nuñez A, et al. A prognostic model based on preoperative MRI predicts overall survival in patients with diffuse gliomas. *Am J Neuroradiol.* 2014;35(6):1096–1102.
36. Romano A, Calabria LF, Tavanti F, et al. Apparent diffusion coefficient obtained by magnetic resonance imaging as a prognostic marker in glioblastomas: correlation with MGMT promoter methylation status. *Eur Radiol.* 2013;23(2):513–520.
37. Zulfiqar M, Yousem DM, Lai H. ADC values and prognosis of malignant astrocytomas: does lower ADC predict a worse prognosis independent of grade of tumor?—A meta-analysis. *Am J Roentgenol.* 2013;200(3):624–629.
38. Hu C, Liu Z, Zhao H, et al. A biochemical comparison of the lung, colonic, brain, renal, and ovarian cancer cell lines using 1H-NMR spectroscopy. *Biosci Rep.* 2020;40(4):BSR20194027.
39. Righi V, Roda JM, Paz J, et al. ^{1}H HR-MAS and genomic analysis of human tumor biopsies discriminate between high and low grade astrocytomas. *NMR Biomed.* 2009;22(6):629–637.
40. Gollapalli K, Ghantasala S, Atak A, et al. Tissue proteome analysis of different grades of human gliomas provides major cues for glioma pathogenesis. *OMICS.* 2017;21(5):275–284.